Title	Motion of patterns in polariton quantum fluids with spin-orbit interaction
Author(s)	Egorov, O. A.; Werner, A.; Liew, Timothy Chi Hin; Ostrovskaya, E. A.; Lederer, F.
Citation	Egorov, O. A., Werner, A., Liew, T. C. H., Ostrovskaya, E. A., & Lederer, F. (2014). Motion of patterns in polariton quantum fluids with spin-orbit interaction. Physical Review B, 89(23), 235302-.
Date	2014
URL	http://hdl.handle.net/10220/20012
Rights	© 2014 American Physical Society. This paper was published in Physical Review B and is made available as an electronic reprint (preprint) with permission of American Physical Society. The paper can be found at the following official DOI: http://dx.doi.org/10.1103/PhysRevB.89.235302. One print or electronic copy may be made for personal use only. Systematic or multiple reproduction, distribution to multiple locations via electronic or other means, duplication of any material in this paper for a fee or for commercial purposes, or modification of the content of the paper is prohibited and is subject to penalties under law.

Motion of patterns in polariton quantum fluids with spin-orbit interaction

O. A. Egorov,[1] A. Werner,[1] T. C. H. Liew,[2] E. A. Ostrovskaya,[3] and F. Lederer[1]

[1]*Institute of Condensed Matter Theory and Solid State Optics, Abbe Center of Photonics, Friedrich-Schiller-Universität Jena, Max-Wien-Platz 1, 07743 Jena, Germany*

[2]*Division of Physics and Applied Physics, Nanyang Technological University, Singapore 637371*

[3]*Nonlinear Physics Centre, Research School of Physics and Engineering, The Australian National University, Canberra, ACT 0200, Australia*

(Received 7 March 2014; revised manuscript received 8 May 2014; published 3 June 2014)

We report on a remarkable effect of pseudospin precession on the collective motion of exciton-polaritons in a microresonator coherently driven by a linearly polarized pump. In particular, we show that hexagonal patterns can undergo a spontaneous symmetry breaking of their polarization and start a uniform motion in the plane of the resonator. Similar to the *optical spin Hall effect*, this becomes possible due to a spin-orbit interaction induced by a longitudinal-transverse splitting (TE-TM splitting) of the photonic resonator mode. We derive a simple analytical expression for the drift velocity of the patterns.

DOI: 10.1103/PhysRevB.89.235302 PACS number(s): 71.36.+c, 42.65.Pc, 42.65.Sf, 42.65.Tg

I. INTRODUCTION

The observation of *strong coupling* between excitons and photons in a high-quality semiconductor microresonator [1] initiated an extensive multidisciplinary study embracing the fields of nonlinear optics, quantum theory, and solid-state physics [2–4]. Unique optical properties, such as nonparabolic dispersion and strong nonlinearity, are derived from the hybrid light-matter nature of the elementary excitations, called *cavity exciton-polaritons*. The extremely small effective masses of these composite bosons allow for the observation of high-temperature nonequilibrium Bose-Einstein condensation [3,5]. Moving exciton-polaritons can behave like a quantum fluid, sharing the properties of superfluidity [4,6,7]. Also the turbulent emission of quantized vortices and the nucleation of dark solitons have been observed [8,9]. A unique interplay between the nonparabolic dispersion and parametric effects allows for the formation of polariton droplets moving in the plane of a coherently driven semiconductor microresonator [10–12].

The pseudospin, inherited from the spins of a quantum well (QW) exciton and a cavity photon, induces a new degree of freedom into the dynamics of exciton-polaritons [2,13]. For instance, it gives rise to polarization multistability [14]. Moreover, due to the longitudinal-transverse (TE-TM) splitting of the polaritons [15], the pseudospin of the ballistic exciton-polariton experiences a precession, whose rotation velocity depends on both the direction and the modulus of the polariton momentum $\mathbf{k}$ [13,16–18]. Thus, TE-TM splitting induces an effective Rashba-type *spin-orbit interaction* [13], which gives rise to the spatial separation of spins of intracavity polaritons, e.g., the *optical spin Hall effect* (OSHE) [16,17]. As a result, spin currents can coherently propagate over 100 μm perpendicular to the exciton-polariton flows [17], or circularly polarized ring patterns can form under highly nonresonant local excitation [19]. In general, the *spin-orbit interaction* couples the spin with the translational motion and underpins many fundamental phenomena in physics, such as the *spin Hall effect* (SHE) of electrons in solids [20,21] or the *SHE of light* known from pure photonic systems [22,23]. However, so far spin currents in polariton systems with spin-orbit interactions have not been linked to the density currents.

In this paper we demonstrate theoretically that the directionally dependent pseudospin precession can result in a collective motion of polariton patterns in a microresonator coherently driven by a linearly polarized optical pump [Fig. 1(a)]. It is remarkable that, contrary to conventional OSHE [16,17], the pseudospin precession induces a directional current of polariton density rather than a spin current. As an example we consider a hexagonal pattern which starts uniformly moving provided that the TE-TM mode splitting is taken into account. Hexagonal patterns have been studied recently for the scalar case [24,25] in the vicinity of the lower polariton branch [Fig.1(b)] and have been observed experimentally in a double-cavity configuration [26].

In general, the physics behind pattern formation is well understood in a wide variety of nonequilibrium dissipative systems (for a review, see [27]) such as cavities with a Kerr nonlinearity [28,29] or a saturable absorber [30] and semiconductor resonators [31].

II. MATHEMATICAL MODEL

The widely accepted dimensionless model describes the dynamics of excitons with spin up (Ψ^+) and spin down (Ψ^-) which are directly coupled to cavity photons carrying the right (E^+) and the left (E^-) circular polarizations, respectively [2,6,9,13]:

$$\begin{aligned}&\partial_t E^\pm - i\nabla_\perp^2 E^\pm + [\gamma - i\Omega_p]E^\pm + i\beta(\partial_x \mp i\partial_y)^2 E^\mp \\ &\quad = i\Psi^\pm + E_p^\pm, \\ &\partial_t \Psi^\pm + (\gamma - i\Omega_p + i|\Psi^\pm|^2 + i\alpha|\Psi^\mp|^2)\Psi^\pm = iE^\pm. \quad (1)\end{aligned}$$

The normalization is such that $(\Omega_R/g)|E^\pm|^2$ and $(\Omega_R/g)|\Psi^\pm|^2$ are the photon and exciton numbers per unit area, Ω_R is the Rabi frequency, and g is the interaction constant of excitons with equal spin. The quantity $\Omega_p = (\omega_p - \omega_0)/\Omega_R$ describes the detuning of the pump frequency ω_p from the identical cavity and excitonic resonances ω_0. The cavity and the exciton damping constants are assumed to be equal (γ) and normalized to Ω_R. The TE-TM splitting of the cavity modes gives rise to the linear coupling between right- and left-circular polarizations and is denoted by β [9,13,18,19].

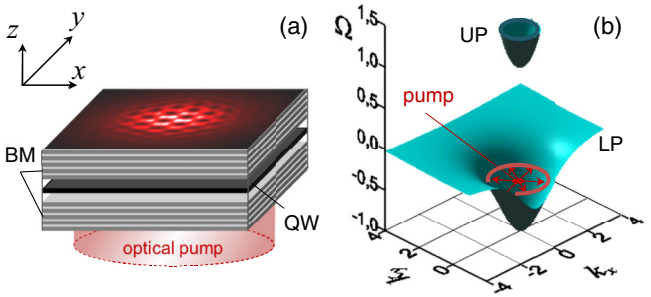

FIG. 1. (Color online) (a) Sketch of the microcavity driven by a coherent optical pump. The semiconductor quantum well (QW) is sandwiched between two Bragg mirrors (BM). (b) Dispersion of the lower (LP) and upper (UP) polaritons.

Also the nonlinear interaction between excitons with different spins is taken into account (parameter α) [9,13,14].

As a guideline for realistic estimates one can use parameters of a microcavity with a single InGaAs/GaAs quantum well: $\hbar\Omega_R \simeq 2.5$ meV, $\hbar g \simeq 10^{-4}$ eV μm^2 (see [6,32]). Therefore, a unit of t corresponds to 0.25 ps, and a unit of the transverse coordinates x, y corresponds to about 1 μm. Assuming the relaxation times of excitons and the cavity lifetime to be 2.5 ps gives $\gamma \simeq 0.1$. Full details of the rescaling into physical units can be found in [33].

III. CIRCULARLY POLARIZED PUMP

We start by discussing the case of a coherent optical pump carrying a right-hand circular polarization, i.e., $E_p^+ = E_p$ and $E_p^- = 0$. Neglecting for now the TE-TM splitting, we can reduce the model (1) to the scalar one. First, we define the eigenstates of the system in the linear limit. Looking for a solution as $\{E,\Psi\} = \mathbf{p}(k)e^{-\gamma t + i[\mathbf{k}\cdot\mathbf{r} - \Omega(k)t]}$ and dropping both the pump and the nonlinear terms, one arrives at the eigenvalue problem for the basis vector $\mathbf{p}(k) = \{e_k, \psi_k\}$ and the eigenfrequency $\Omega(k)$ (for details see [33]). Solution of the eigenvalue problem yields the two branches of the linear polariton dispersion relation,

$$\Omega_{\mathrm{up,lp}}(k) = \tfrac{1}{2}(k^2 \pm \sqrt{4+k^4}), \qquad (2)$$

where $\Omega_{\mathrm{up}}(k)$ [$\Omega_{\mathrm{lp}}(k)$] refers to the upper (lower) polariton branch [see Fig. 1(b)]. Here, $e_k^2 = \{1 + [k^2 - \Omega_{\mathrm{up,lp}}(k)]^2\}^{-1}$ and $\psi_k^2 = 1 - e_k^2$ are the photonic and excitonic components (also known as the Hopfield coefficients [34]), respectively.

Near the bottom of the lower polariton branch the polaritonic dispersion relation is approximately parabolic [see Fig. 1(b)]. Therefore, the arising patterns are expected to resemble those in Kerr cavities [28,29]. Figure 2(a) shows the photonic component of a steady-state *homogeneous solution* (HS) of Eq. (1) under a circularly polarized homogeneous pump ($E_p^+ = E_p$). The HS becomes modulationally unstable provided that the pump amplitude exceeds a critical value. This *modulational instability*(MI) is associated with the parametrical generation of field components with nonzero momenta k. Figure 2(b) presents the linear growth rate $\mathrm{Re}\lambda(k)$ of the unstable perturbations of the form $\sim\exp\{[ik_x x + ik_y y + \lambda(k)t]\}$ as function of their momenta $k = \sqrt{k_x^2 + k_y^2}$ and the

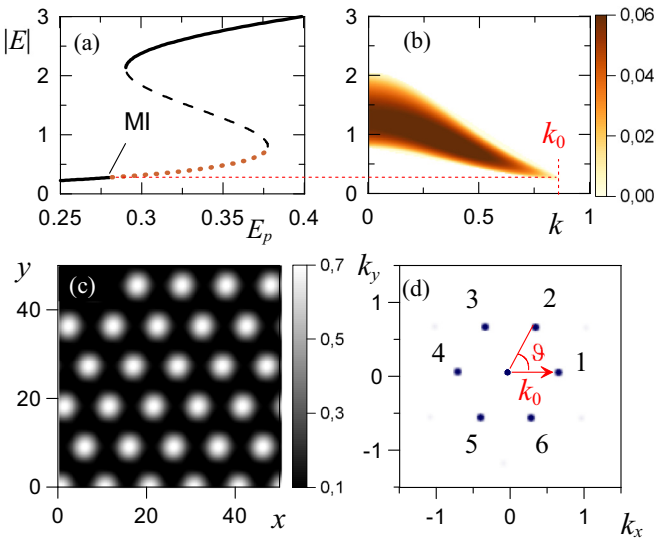

FIG. 2. (Color online) (a) Amplitude $|E|$ of the homogeneous solution (HS) vs the pump amplitude E_p. The dashed lines represent unstable states and MI depicts the bifurcation point of modulational instability. (b) Growth rate (real part of λ) of the unstable perturbation as a function of momentum k and HS amplitude $|E|$. (c) Spatial $|E^+(x,y)|^2$ and (d) the corresponding Fourier profile of the hexagonal pattern calculated for a circularly polarized pump of amplitude $E_p^+ = 0.287$. Other parameters are $\alpha = -0.1$, $\beta = 0.05$, $\Omega_p = -0.5$.

HS amplitude. A broad laser beam launched perpendicular to the plane of the microresonator experiences spontaneous translational symmetry breaking, resulting in the formation of a hexagonal pattern [see Fig. 2(c) and [24,25]]. The six main Fourier components of this hexagonal pattern lie on a circle whose radius is related to the momentum of the maximal MI gain $k_0 \approx k_{\max}$ [Fig. 2(d)].

IV. MOVING HEXAGONAL PATTERNS

The physics changes drastically for a linearly polarized optical pump, i.e., $E_p = E_p^+ = E_p^-$. Both polarization components are comparable and interact via linear (TE-TM splitting β) and nonlinear (α) coupling mechanisms. The polarization state of the polaritons can be represented by the Stokes vector, where $\rho = S_z/S_0$ describes its circular polarization degree, $S_z = |E^+|^2 - |E^-|^2$ and $S_0 = |E^+|^2 + |E^-|^2$.

By virtue of direct numerical simulations of the two-component model (1) we study the formation of hexagonal patterns in the presence of polarization effects. The solution loses the linear polarization imprinted by the pump. As a result the bright peaks of the hexagonal pattern split into tightly bound spots carrying opposite circular polarizations [Figs. 3(a) and 3(b)]. We note that the spontaneous breaking of the linear polarization can be induced by the cross-spin nonlinear coupling term α, as has been shown for localized solutions [35].

It is remarkable that the vectorial hexagonal pattern starts a uniform motion in the resonator plane provided that the TE-TM mode splitting ($\beta \neq 0$) is taken into account [Figs. 3(c) and 3(d)]. Apparently, like in the OSHE [16,17], the pseudospins of the exciton-polaritons experience directionally

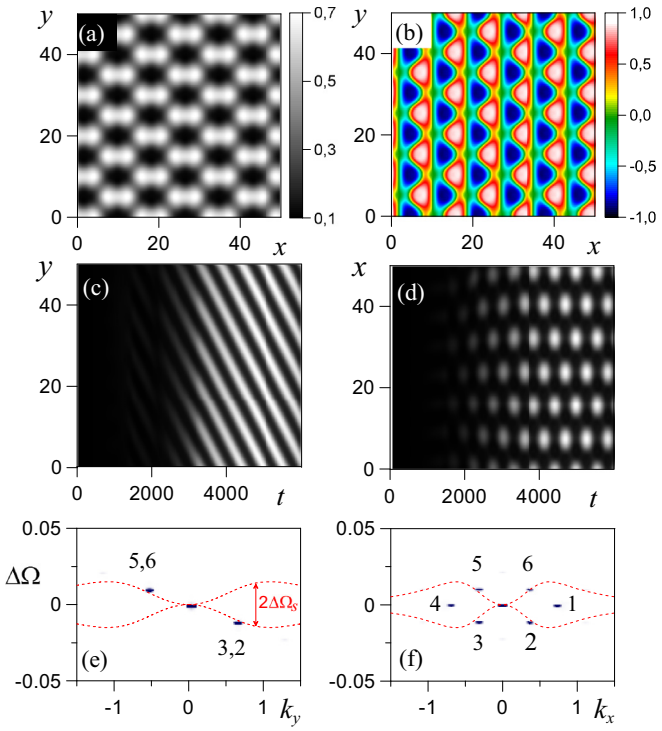

FIG. 3. (Color online) (a) Intensity profile $I = |E^+|^2 + |E^-|^2$ of the hexagonal pattern and (b) its circular polarization degree ρ calculated for a linearly polarized pump of amplitude $E_p^+ = E_p^- = 0.283$. Temporal evolution of (c) the y and (d) x intensity profiles of the moving hexagonal pattern. Fourier components of the moving hexagonal pattern along (e) the y and (f) x axes. The red dashed lines depict the frequency shifts given by Eq. (10). Other parameters are $\alpha = -0.1$, $\beta = 0.05$.

dependent precessions whose rotation velocities and rotation directions are different for different Fourier components of the hexagonal pattern. Thus, the Fourier components of the hexagonal pattern [depicted by points 1–6 in Fig. 2(d)] acquire new phases which slowly depend on time. These relative phases between the Fourier components are directly related to the position of the intensity maxima. Therefore, one expects that the peaks of the pattern will start drifting.

To illustrate this dynamics we performed temporal Fourier transformations of the moving hexagonal pattern and plotted the results in Figs. 3(e) and 3(f). Both Fourier components with negative $k_y < 0$ (depicted by 5 and 6) are blueshifted, whereas the two components on the opposite side ($k_y > 0$, depicted by 2 and 3) are redshifted. Thus, the Fourier components of the moving hexagonal pattern belong to a plane which is tilted along the axis k_y. If the frequency shift $\Delta\Omega_s$ is known, the velocity of the hexagonal pattern can be found as

$$v = \Delta\Omega_s/k_y = \Delta\Omega_s/[k_0 \sin(\theta)]. \tag{3}$$

Below we show that the frequency shift $\Delta\Omega_s$ is associated with the TE-TM splitting of the polaritons. For an analytical study we represent the hexagonal pattern as a superposition of the six main spectral components and a homogeneous background

$$\left|\begin{matrix} E^\pm \\ \Psi^\pm \end{matrix}\right| = \mathbf{p}(0)A_0^\pm + \sum_{j=1}^{6} \mathbf{p}(k_0)A_j^\pm e^{i(\mathbf{k}_j+\Delta\mathbf{k}_j)\cdot\mathbf{r} - i\Delta\Omega_j t}, \tag{4}$$

where the momenta of these components are $\mathbf{k}_j = \{k_0\cos\theta_j, k_0\sin\theta_j\}$ and $\theta_j = (j-1)\pi/3$ [see Fig. 2(d)]. Expression (4) is written in the polaritonic basis disregarding the upper-polariton branch, where $\mathbf{p}(k_0)$ represents the basis vectors of the lower polaritons. The TE-TM splitting induces corrections to the momenta $\Delta\mathbf{k}_j$ and the frequencies $\Delta\Omega_j$ of the spectral components. It is reasonable to assume that the amplitudes A_j remain constant because the TE-TM splitting term is small. Then, inserting the ansatz (4) into Eq. (1), we derive the set of coupled equations

$$\begin{aligned}&[\Delta\Omega_j - \Omega_{lp}(\mathbf{k}_j + \Delta\mathbf{k}_j)]A_j^\pm + N_j^\pm \\ &\quad = \beta[i(k_{xj} + \Delta k_{xj}) \pm (k_{yj} + \Delta k_{yj})]^2 e_{k_0}^2 A_j^\mp,\end{aligned} \tag{5}$$

where the nonlinear mixing terms have the form $N_j^\pm \sim \sum_{m=0}^{6}\sum_{n=0}^{6}(A_m^\pm A_n^{*\pm} + \alpha A_m^\mp A_n^{*\mp})A_{j-m+n}^\pm$ and A_{j-m+n} is the amplitude of the mode $\mathbf{k}_j - \mathbf{k}_m + \mathbf{k}_n$. By deriving Eq. (5) both the phase- and the frequency-matching conditions were assumed. The phase-matching conditions can be reduced to the following set of equations:

$$\begin{aligned}&\Delta\mathbf{k}_1 = -\Delta\mathbf{k}_4, \quad \Delta\mathbf{k}_2 = -\Delta\mathbf{k}_5, \quad \Delta\mathbf{k}_3 = -\Delta\mathbf{k}_6, \\ &\Delta\mathbf{k}_1 = \Delta\mathbf{k}_2 + \Delta\mathbf{k}_6,\end{aligned} \tag{6}$$

whereas the frequency-matching conditions read

$$\begin{aligned}&\Delta\Omega_1 = -\Delta\Omega_4, \quad \Delta\Omega_2 = -\Delta\Omega_5, \quad \Delta\Omega_3 = -\Delta\Omega_6, \\ &\Delta\Omega_1 = \Delta\Omega_2 + \Delta\Omega_6.\end{aligned} \tag{7}$$

In the framework of a perturbation theory we are looking for small corrections to the frequencies $\Delta\Omega_j$ and wave vectors $\Delta\mathbf{k}_j$ of the hexagonal pattern induced by the TE-TM splitting, where $\beta \neq 0$ is a small parameter. The first-order correction can be obtained from Eq. (5):

$$\begin{aligned}&\left[\Delta\Omega_j - 2\Omega'_{lp}\left(k_0^2\right)(k_{xj}\Delta k_{xj} + k_{yj}\Delta k_{yj})\right]A_j^\pm \\ &\quad = \beta e_{k_0}^2 (ik_{xj} \pm k_{yj})^2 A_j^\mp.\end{aligned} \tag{8}$$

Here we perform a Taylor expansion of the lower-polariton dispersion $\Omega'_{lp}(k_0^2) \equiv \partial\Omega_{lp}(k^2)/\partial(k^2)|_{k^2=k_0^2} = \frac{1}{2}(1 - k_0^2/\sqrt{4+k_0^4})$. The solvability condition of the linear system (8) gives the expression for the frequency shifts:

$$\begin{aligned}\Delta\Omega_j &= 2\Omega'_{lp}\left(k_0^2\right)(k_{xj}\Delta k_{xj} + k_{yj}\Delta k_{yj}) \\ &\quad \pm \tfrac{1}{2}\beta k_0^2\left(1 - k_0^2/\sqrt{4+k_0^4}\right).\end{aligned} \tag{9}$$

The Fourier components of the moving hexagonal pattern (Fig. 3) satisfy Eq. (9). Indeed, the relations $\Delta\Omega_1 = \Delta\Omega_4 = 0$ are valid provided that $\Delta k_{x1} = \frac{1}{2}\beta k_0$ and $\Delta k_{x4} = -\frac{1}{2}\beta k_0$. The frequency shifts $\Delta\Omega_{2,3} = -\Delta\Omega_{5,6} = -\Delta\Omega_s$ can be obtained from Eq. (9) provided that the wave vectors satisfy $\Delta k_{x2,5}/\Delta k_{y2,5} = -\Delta k_{x3,6}/\Delta k_{y3,6} = -\tan(\pi/3) = -\sqrt{3}$. In this case the frequency shift is given by

$$\Delta\Omega_s = \tfrac{1}{2}\beta k_0^2\left(1 - k_0^2/\sqrt{4+k_0^4}\right). \tag{10}$$

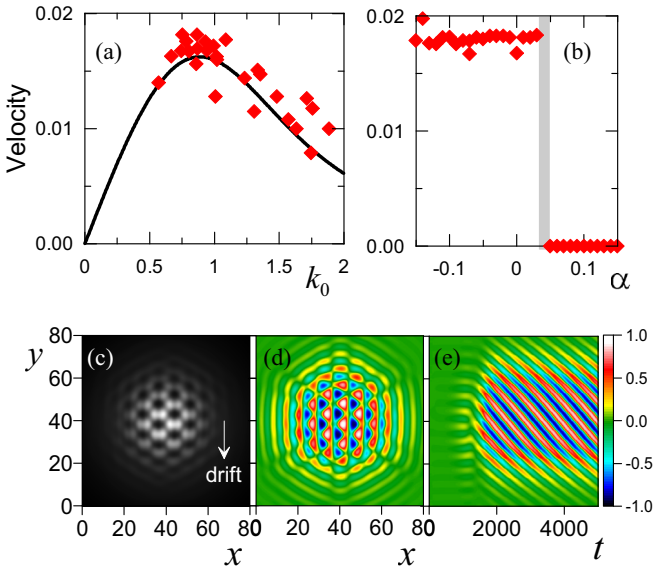

FIG. 4. (Color online) (a) The velocity of the pattern vs its main wave vector k_0. The solid line represents the results of the analytical approximation (3). The points depict the results of direct numerical simulation of Eq. (1) for different parameters. (b) The velocity of the pattern vs the parameter α. (c) The intensity profile, (d) polarization profiles, and (e) temporal dynamics of the moving hexagonal pattern driven by a linearly polarized Gaussian pump with diameter 120 (about 120 μm) and amplitudes $E_p^+ = E_p^- = 0.31$. Other parameters $\Omega_p = -0.45$, $\alpha = -0.1$, $\beta = 0.05$. See also the Supplemental Material [36].

We note that the obtained corrections explicitly satisfy both the phase-matching [Eq. (6)] and frequency-matching [Eq. (7)] conditions.

The frequency shift given by Eq. (10) is equal to half of the frequency splitting between the TE and TM photonic modes [dashed lines in Figs. 3(e) and 3(f)]. First, it grows quadratically with the momenta and reaches the maximal value in the vicinity of the inflection point of the lower-polariton branch [18].

Using the original model (1), we modeled the hexagonal pattern formation numerically for different values of the pump amplitudes and detunings. Then the velocities of the resulting hexagonal patterns were plotted versus their main momentum k_0 [red diamonds in Fig. 4(a)]. There is good agreement between the analytical expression (3) and the direct numerical simulations. Moving hexagonal patterns exist mainly for negative values of the cross-spin nonlinear coefficient α and transform into resting patterns provided that the parameter α exceeds some positive threshold [see Fig. 4(b)].

A moving hexagonal pattern also exists for the more realistic case of a spatially localized pump [Figs. 4(c)–4(e) and Supplemental Material [36]]. Depending on the initial conditions, the pattern starts moving either along the x or y direction when the pump is linearly polarized in the x direction. The calculated value of the drift velocity corresponds to a physical value of about 0.1 μm/ps.

V. CONCLUSIONS

In conclusion, by means of numerical and analytical studies we have shown that the spin degree of freedom can induce transversal motion of an intensity pattern in semiconductor microresonators operating in the strong-coupling regime. Similar to the optical spin Hall effect, this drift is induced by the directionally dependent pseudospin precession of polaritons. We emphasize that these phenomena are generic and can be expected to occur in other nonlinear systems with a spin-orbit-interaction mechanism, for instance, in atomic Bose-Einstein condensates with gauge fields [37], two-component optical resonators with Kerr nonlinearity [38], and wide-aperture vertical-cavity surface-emitting lasers (VCSELs) with TE-TM mode splitting [39].

ACKNOWLEDGMENT

This work was supported by the Thuringian Ministry of Education, Science and Culture through Project. No. B514-11027.

[1] C. Weisbuch, M. Nishioka, A. Ishikawa, and Y. Arakawa, Phys. Rev. Lett. **69**, 3314 (1992).
[2] B. Deveaud, *The Physics of Semiconductor Microcavities* (Wiley-VCH, Weinheim, 2007).
[3] H. Deng, H. Haug, and Y. Yamamoto, Rev. Mod. Phys. **82**, 1489 (2010).
[4] I. Carusotto and C. Ciuti, Rev. Mod. Phys. **85**, 299 (2013).
[5] J. Kasprzak, M. Richard, S. Kundermann, A. Baas, P. Jeambrun, J. M. Keeling, F. M. Marchetti, M. H. Szymanska, R. Andre, J. L. Staehli, V. Savona, P. B. Littlewood, B. Deveaud, and L. S. Dang, Nature (London) **443**, 409 (2006).
[6] I. Carusotto and C. Ciuti, Phys. Rev. Lett. **93**, 166401 (2004).
[7] A. Amo, J. Lefrere, S. Pigeon, C. Adrados, C. Ciuti, I. Carusotto, R. Houdre, E. Giacobino, and A. Bramati, Nat. Phys. **5**, 805 (2009).
[8] A. Amo, S. Pigeon, D. Sanvitto, V. G. Sala, R. Hivet, I. Carusotto, F. Pisanello, G. Leménager, R. Houdré, E. Giacobino, C. Ciuti, and A. Bramati, Science **332**, 1167 (2011).
[9] H. Flayac, D. D. Solnyshkov, and G. Malpuech, Phys. Rev. B **83**, 193305 (2011).
[10] A. Amo, D. Sanvitto, F. P. Laussy, D. Ballarini, E. del Valle, M. D. Martin, A. Lemaître, J. Bloch, D. N. Krizhanovskii, M. S. Skolnick, C. Tejedor, and L. Vina, Nature (London) **457**, 291 (2009).
[11] O. A. Egorov, A. V. Gorbach, F. Lederer, and D. V. Skryabin, Phys. Rev. Lett. **105**, 073903 (2010).
[12] M. Sich, D. Krizhanovskii, M. S. Skolnick, A. V. Gorbach, R. Hartley, D. Skryabin, E. Cerda-Mendez, K. Biermann, R. Hey, and P. Santos, Nat. Photonics **6**, 50 (2012).
[13] I. A. Shelykh, A. V. Kavokin, Y. G. Rubo, T. C. H. Liew, and G. Malpuech, Semicond. Sci. Technol. **25**, 013001 (2010).
[14] N. A. Gippius, I. A. Shelykh, D. D. Solnyshkov, S. S. Gavrilov, Y. G. Rubo, A. V. Kavokin, S. G. Tikhodeev, and G. Malpuech, Phys. Rev. Lett. **98**, 236401 (2007).
[15] G. Panzarini, L. C. Andreani, A. Armitage, D. Baxter, M. S. Skolnick, V. N. Astratov, J. S. Roberts, A. V. Kavokin, M. R.

Vladimirova, and M. A. Kaliteevski, Phys. Rev. B **59**, 5082 (1999).
[16] A. Kavokin, G. Malpuech, and M. Glazov, Phys. Rev. Lett. **95**, 136601 (2005).
[17] C. Leyder, M. Romanelli, J. P. Karr, E. Giacobino, T. C. H. Liew, M. M. Glazov, A. V. Kavokin, G. Malpuech, and A. Bramati, Nat. Phys. **3**, 628 (2007).
[18] A. Amo, T. C. H. Liew, C. Adrados, E. Giacobino, A. V. Kavokin, and A. Bramati, Phys. Rev. B **80**, 165325 (2009).
[19] E. Kammann, T. C. H. Liew, H. Ohadi, P. Cilibrizzi, P. Tsotsis, Z. Hatzopoulos, P. G. Savvidis, A. V. Kavokin, and P. G. Lagoudakis, Phys. Rev. Lett. **109**, 036404 (2012).
[20] M. I. Dyakonov and V. I. Perel', Phys. Lett. A **35**, 459 (1971).
[21] Y. K. Kato, R. C. Myers, A. C. Gossard, and D. D. Awschalom, Science **306**, 1910 (2004).
[22] V. S. Liberman and B. Ya. Zel'dovich, Phys. Rev. A **46**, 5199 (1992).
[23] K. Y. Bliokh, A. Niv, V. Kleiner, and E. Hasman, Nat. Photonics **2**, 748 (2008).
[24] M. H. Luk, Y. C. Tse, N. H. Kwong, P. T. Leung, P. Lewandowski, R. Binder, and S. Schumacher, Phys. Rev. B **87**, 205307 (2013).
[25] H. Saito, T. Aioi, and T. Kadokura, Phys. Rev. Lett. **110**, 026401 (2013).
[26] V. Ardizzone, P. Lewandowski, M. H. Luk, Y. C. Tse, N. H. Kwong, A. Lücke, M. Abbarchi, E. Baudin, E. Galopin, J. Bloch, A. Lemaitre, P. T. Leung, P. Roussignol, R. Binder, J. Tignon, and S. Schumacher, Sci. Rep. **3**, 3016 (2013).
[27] M. C. Cross and P. C. Hohenberg, Rev. Mod. Phys. **65**, 851 (1993).
[28] L. A. Lugiato and R. Lefever, Phys. Rev. Lett. **58**, 2209 (1987).
[29] D. Gomila and P. Colet, Phys. Rev. E **76**, 016217 (2007).
[30] G. K. Harkness, W. J. Firth, G.-L. Oppo, and J. M. McSloy, Phys. Rev. E **66**, 046605 (2002).
[31] T. Maggipinto, M. Brambilla, and W. J. Firth, IEEE J. Quantum Electron. **39**, 206 (2003).
[32] A. Baas, J. P. Karr, H. Eleuch, and E. Giacobino, Phys. Rev. A **69**, 023809 (2004).
[33] O. A. Egorov and F. Lederer, Phys. Rev. B **87**, 115315 (2013).
[34] J. J. Hopfield, Phys. Rev. **112**, 1555 (1958).
[35] A. Werner, O. A. Egorov, and F. Lederer, Phys. Rev. B **85**, 115315 (2012).
[36] See Supplemental Material at http://link.aps.org/supplemental/10.1103/PhysRevB.89.235302 to view the dynamics of both intensity (HexagonIntensity.avi) and polarization (HexagonPolarization.avi) profiles of the moving hexagonal pattern. See the Fig. 4 caption for the details.
[37] Y. J. Lin, K. Jiménez-García, and I. B. Spielman, Nature (London) **471**, 83 (2011).
[38] M. Hoyuelos, P. Colet, M. San Miguel, and D. Walgraef, Phys. Rev. E **58**, 2992 (1998).
[39] I. V. Babushkin, M. Schulz-Ruhtenberg, N. A. Loiko, K. F. Huang, and T. Ackemann, Phys. Rev. Lett. **100**, 213901 (2008).